

Supporting Information

Design, Synthesis, and Enzyme Kinetic Evaluation of Oxadiazole Derivatives as Nucleoside Triphosphate Diphosphohydrolase (NTPDase) Inhibitors: An Integrated *In Vitro* and *In Silico* Approach

Syed Zaighum Abbas¹, Zaman Ashraf^{2, *}, Sadia Roshan³, Kalsoom Sughra⁴, Muhammad Arslan Rahat⁵, Imran Shakir^{6, *}, Muhammad Latif^{2, 7, 8*}

¹Department of Chemistry, Allama Iqbal Open University, Islamabad-44000, Pakistan; realzaghham@hotmail.com (S.Z.A.)

²Department of Chemistry, Rawalpindi Women University, Rawalpindi-46300 Pakistan; zaman.ashraf@rwu.edu.pk (Z.A.)

³Department of Zoology, University of Gujrat, Gujrat-50700, Pakistan; sadia.roshan@uog.edu.pk (S.R.)

⁴Department of Biochemistry and Biotechnology, University of Gujrat, Gujrat 50700, Pakistan; sughra@uog.edu.pk (K.S.)

⁵Department of Chemistry, University of Massachusetts, Amherst, Massachusetts 01003, United States; mrahat@umass.edu (M.A.R.)

⁶Department of Physics, Faculty of Science, Islamic University of Madinah, Madinah, 42351, Saudi Arabia; imranskku@gmail.com (I.S.)

⁷Centre for Genetics and Inherited Diseases (CGID), Taibah University, Madinah, Saudi Arabia; mmuradkhan@taibahu.edu.sa (M.L.)

⁸Department of Basic Medical Sciences, College of Medicine, Taibah University, Madinah, Saudi Arabia; mmuradkhan@taibahu.edu.sa (M.L.)

*Correspondence: zaman.ashraf@rwu.edu.pk (Z.A.); mmuradkhan@taibahu.edu.sa (M.L.); Telephone: +923484038134 (M.L.)

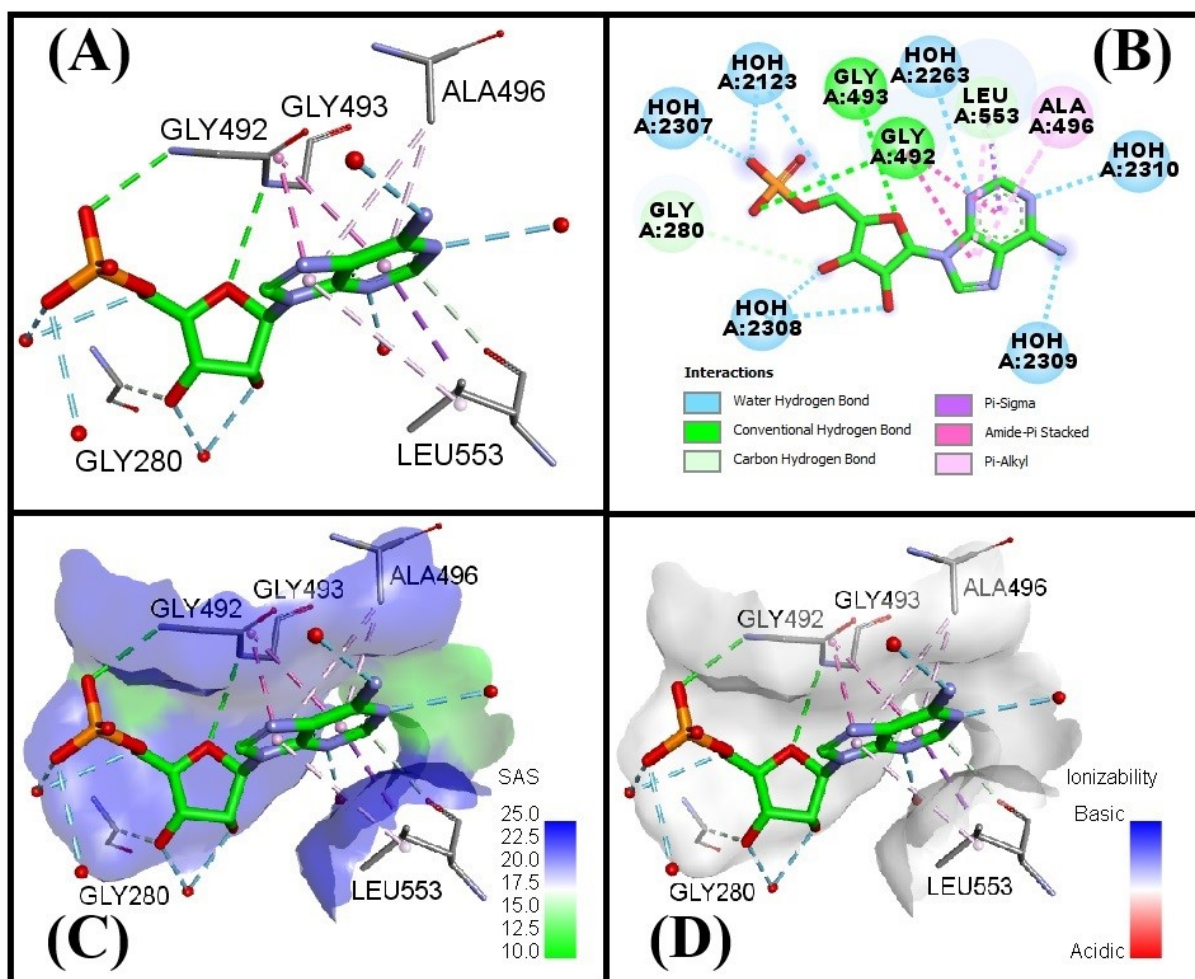


Figure S1. Binding pocket analysis for NTPDase3 containing co-crystallized ligand **Amp700** (green); **(A)** 3D diagram for ligand's interaction, **(B)** 2D diagram for ligand interactions, **(C)** Solvent accessibility surface, **(D)** Ionizability surface.

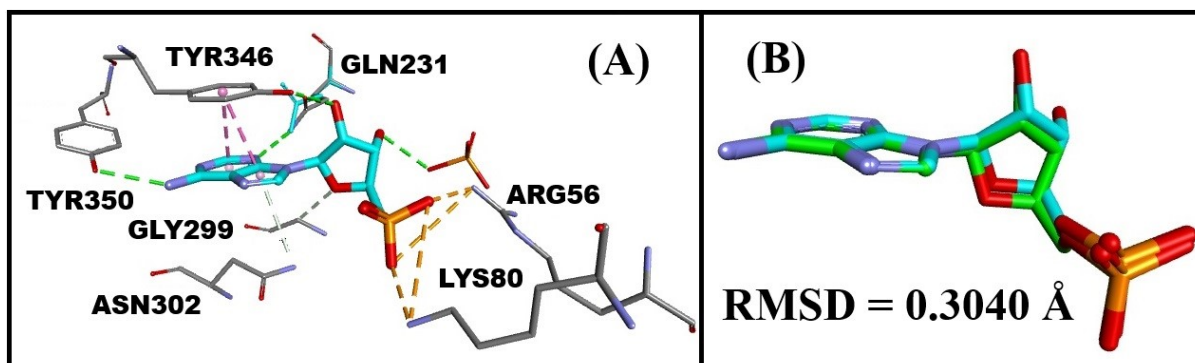


Figure S2. Docking validation for NTPDase1 (A) 3D diagram for redocked ligand **Amp** (cyan) (B) Determination of RMSD using co-crystallized (green) and redocked (cyan) **Amp** ligand.

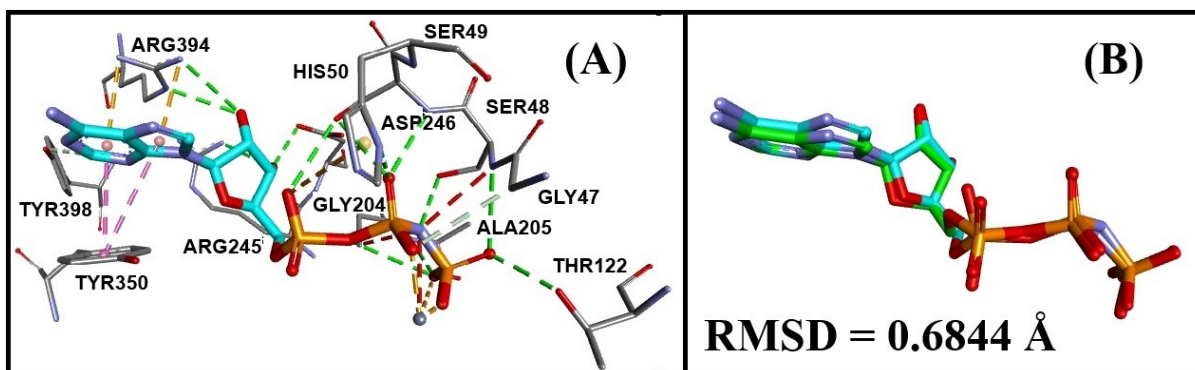


Figure S3. Docking validation for NTPDase2 (A) 3D diagram for redocked ligand **Anp** (cyan) (B) Determination of RMSD using co-crystallized (green) and redocked (cyan) **Anp** ligand.

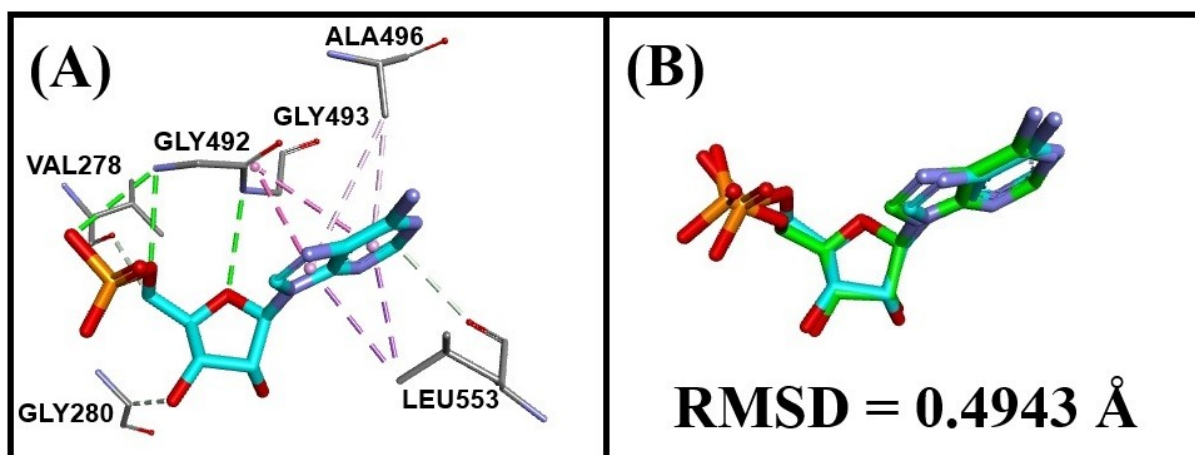


Figure S4. Docking validation for NTPDase3 (A) 3D diagram for redocked ligand **Amp** (cyan) (B) Determination of RMSD using co-crystallized (green) and redocked (cyan) **Amp** ligand.

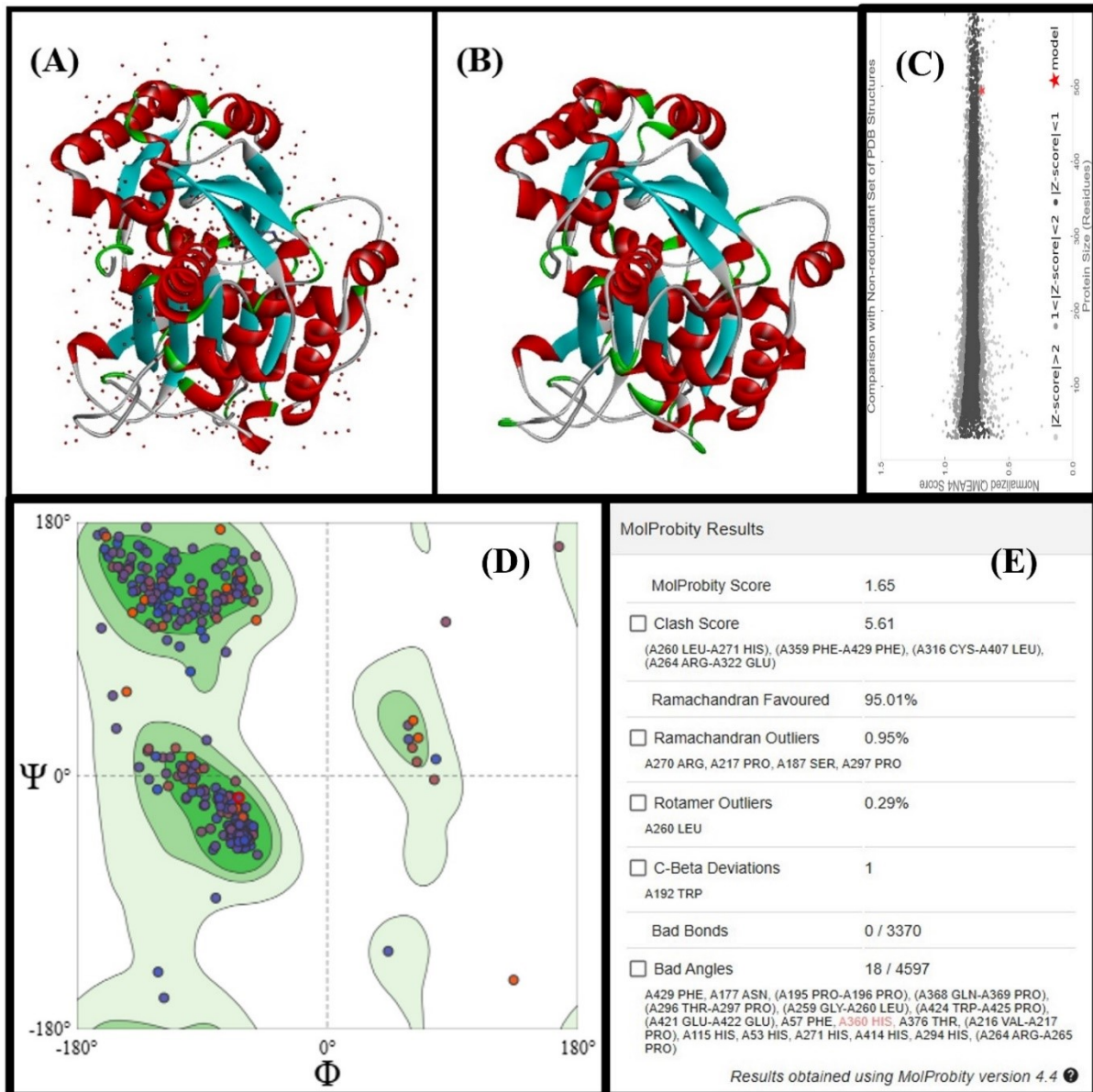


Figure S5. Homology modelling: **(A)** 3CJ9 (NTPDase2) selected for homology modelling, **(B)** NTPDase8 acquired as a homology model, **(C)** Z score, **(D)** Ramachandran plot, **(E)** MolProbity results for the reliability of the homology model.

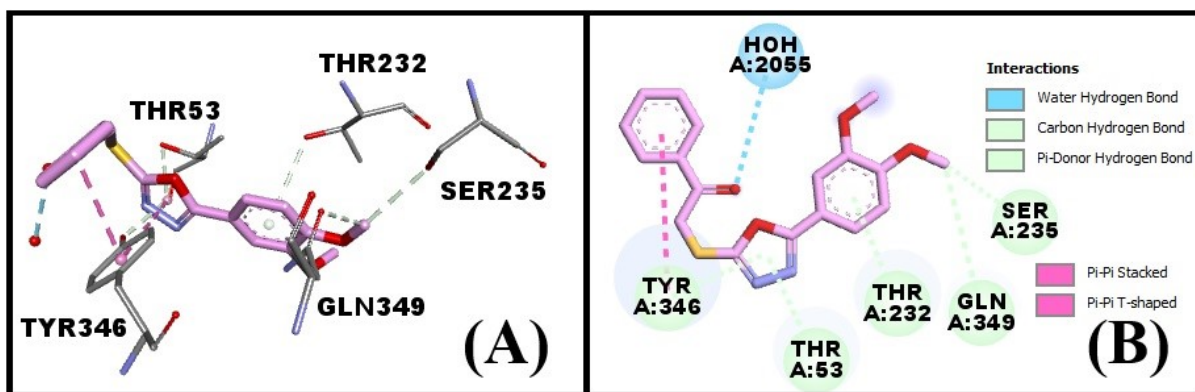


Figure S6. The ligand **7g** (pink) docked on NTPDase1 (4BRQ); **(A)** 3D interactions, **(B)** 2D interactions.

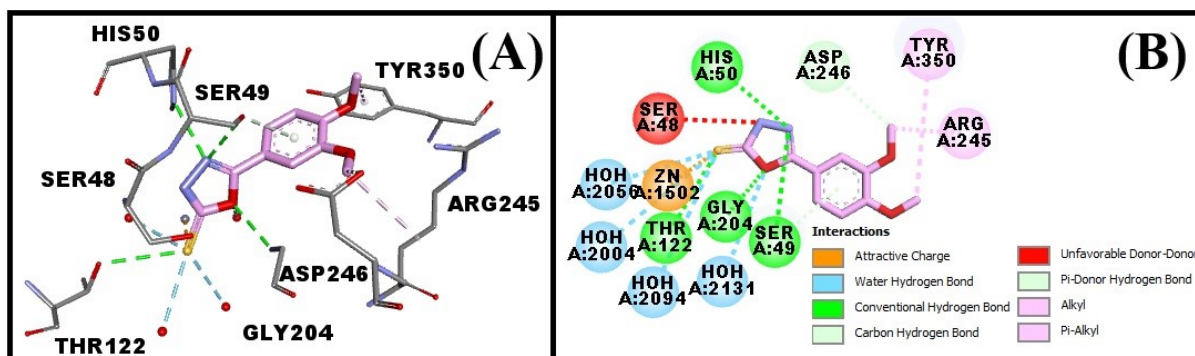


Figure S7. The ligand 4 (Thiol, pink) docked on NTPDase2 (4BR5); (A) 3D interaction, (B) 2D interaction.

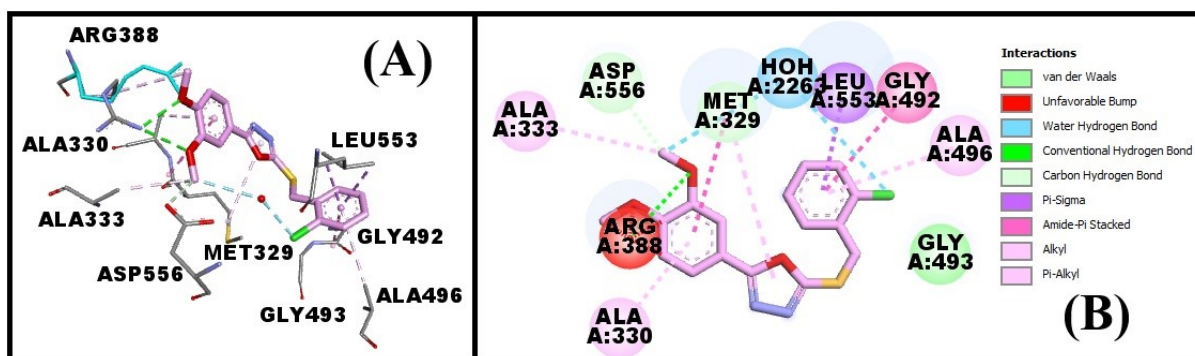


Figure S8. The ligand **7d** (pink) docked on NTPDase3 (4A59); **(A)** 3D interaction, **(B)** 2D interaction.

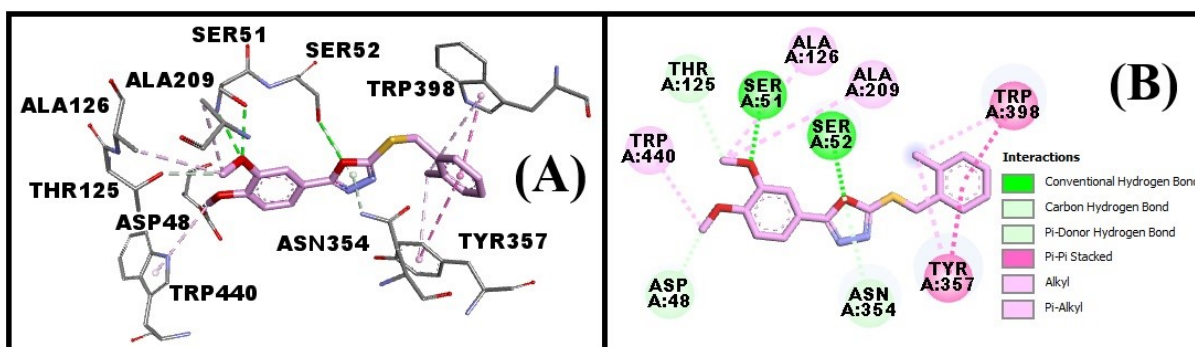


Figure S9. Ligand **7c** (pink) docked on NTPDase8; (A) 3D interaction, (B) 2D interaction. There was no redocked standard used for NTPDase 8, as it was acquired from homology modelling. The **7a-7g** series derivatives, especially **7c**, **7d**, and **7f**, could serve as promising candidates for further refinement and biological testing against NTPDase8.

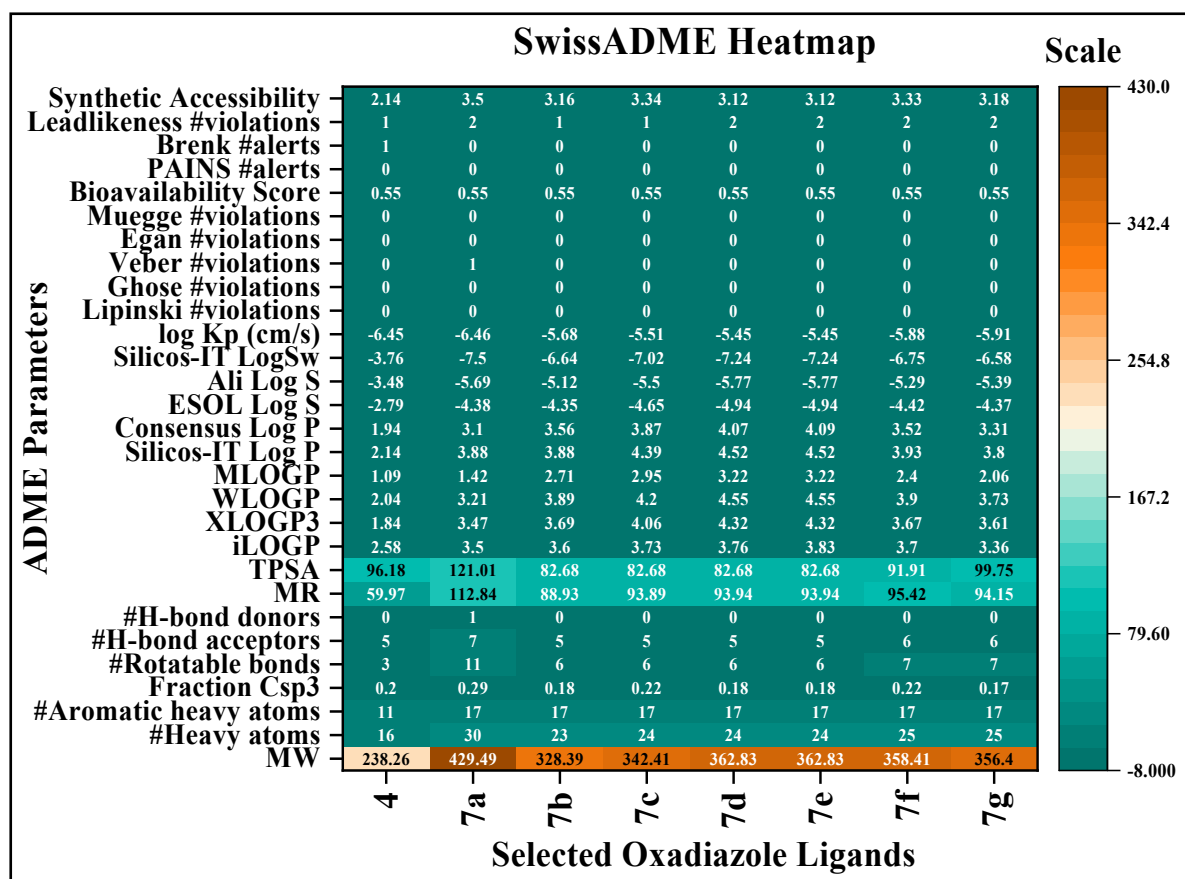


Figure S10. Heat Map for SwissADME Parameters of the Oxadiazole Compounds.

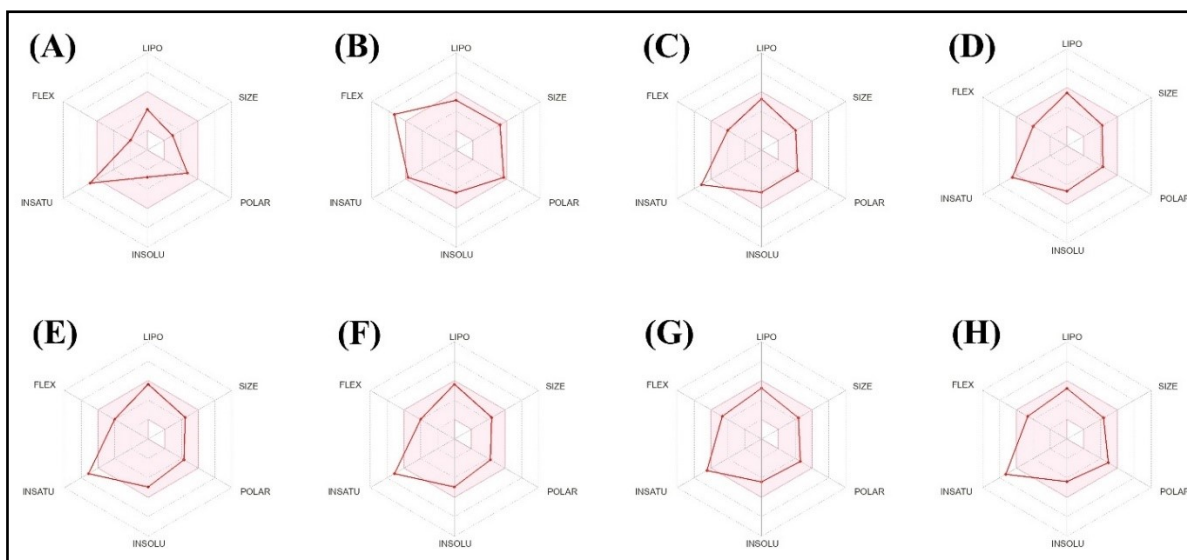
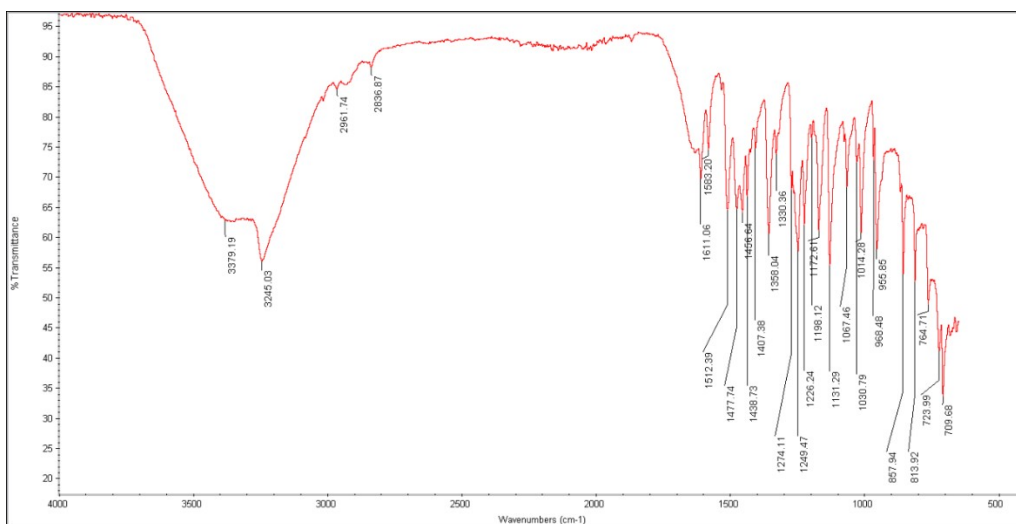
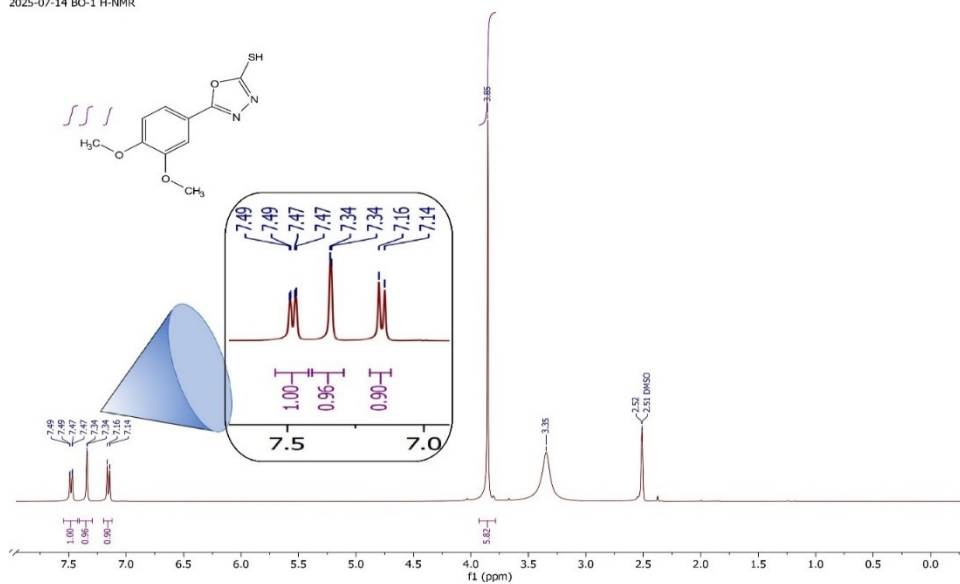


Figure S11. Spiderweb plots for the Oxadiazole Compounds; (A) 4, (B) 7a, (C) 7b, (D) 7c, (E) 7d, (F) 7e, (G) 7f, (H) 7g.



2025-07-14 BO-1 H-NMR 1.fid
2025-07-14 BO-1 H-NMR



BO-1 C-13 NMR 1.fid
BO-1 C-13 NMR

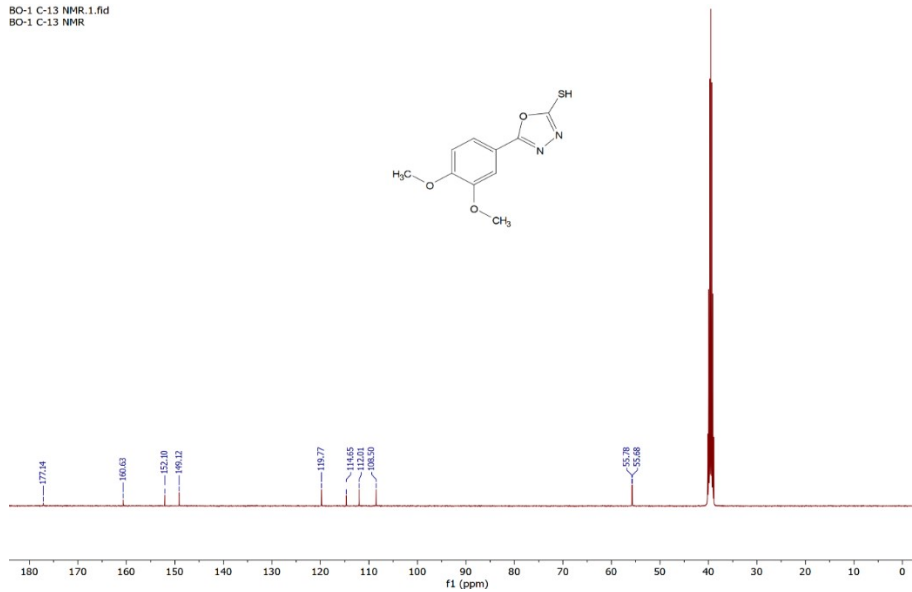
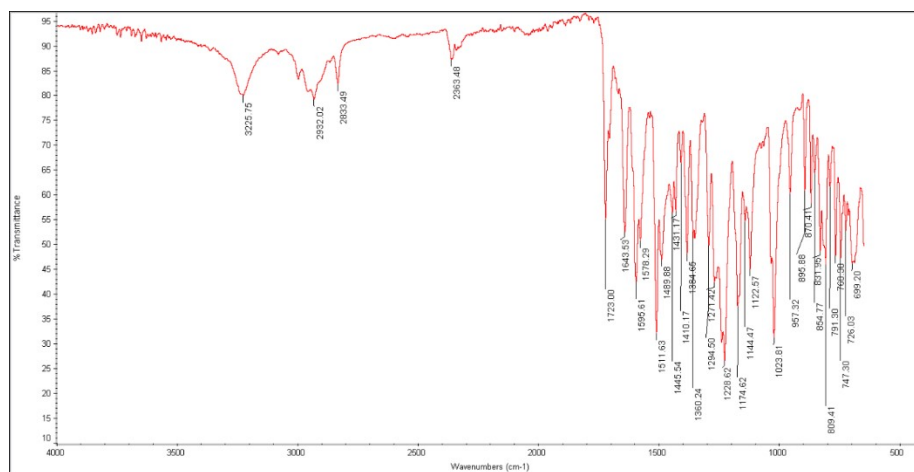
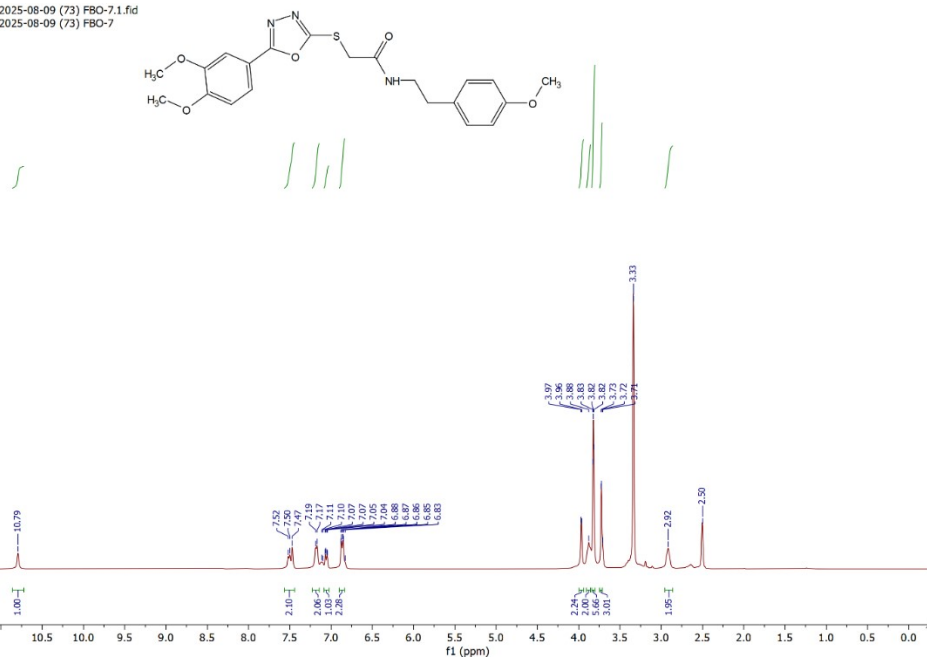


Figure S12: FT-IR, ¹H-, and ¹³C-NMR spectra of compound 4.



2025-08-09 (73) FBO-7.1.fid
2025-08-09 (73) FBO-7



2025-08-09 (73) FBO-7 C-13.1.fid
2025-08-09 (73) FBO-7 C-13

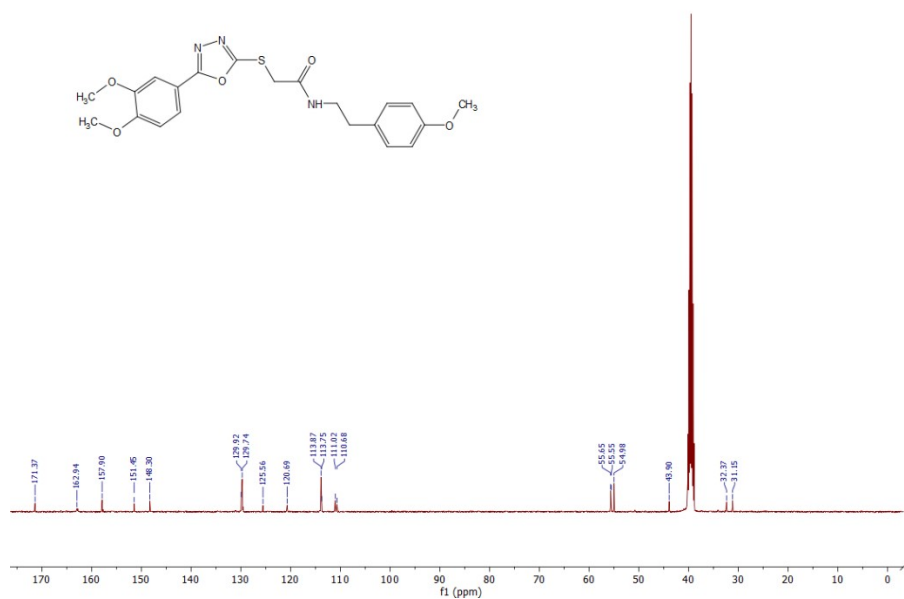
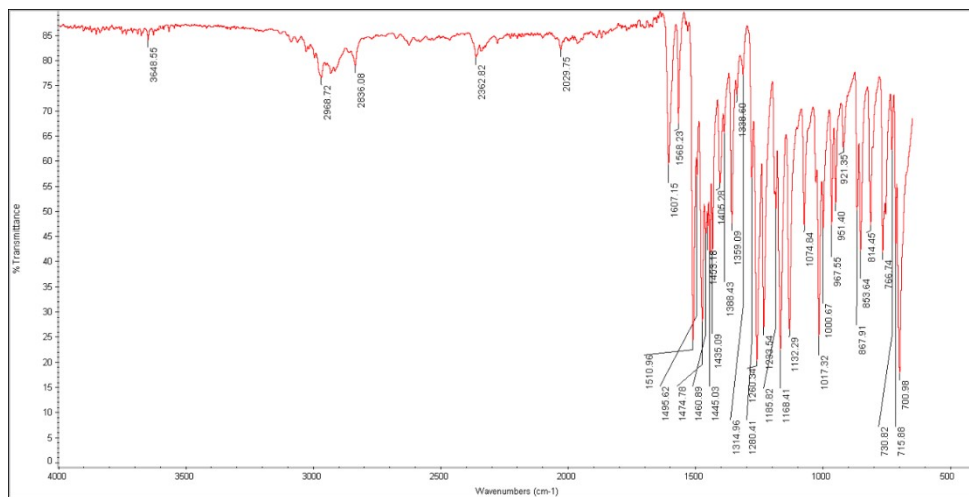
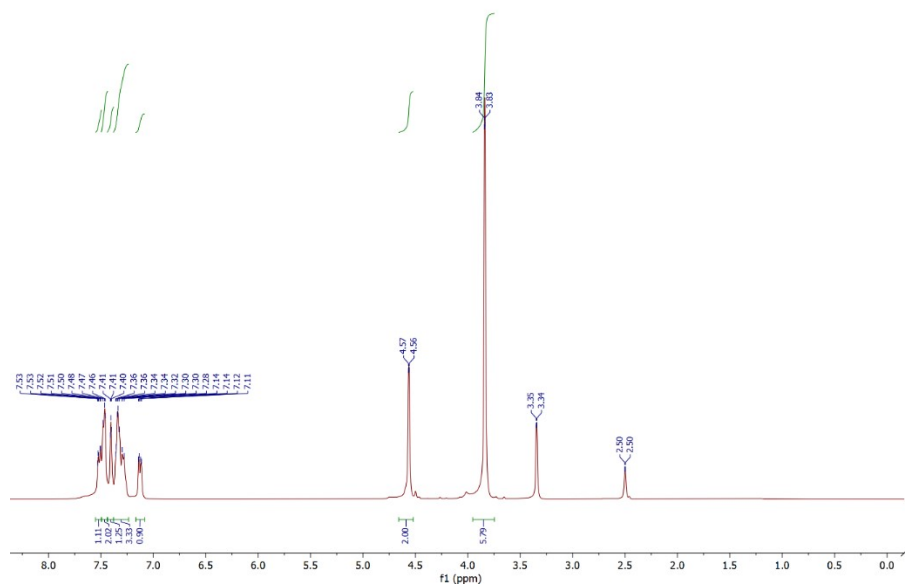


Figure S13: FT-IR, ^1H -, and ^{13}C -NMR spectra of compound **7a**.



2025-07-19 (71).1.fid
2025-07-19 (71)



2025-07-19 FBO-10 (71) C-13.1.fid
2025-07-19 FBO-10 (71) C-13

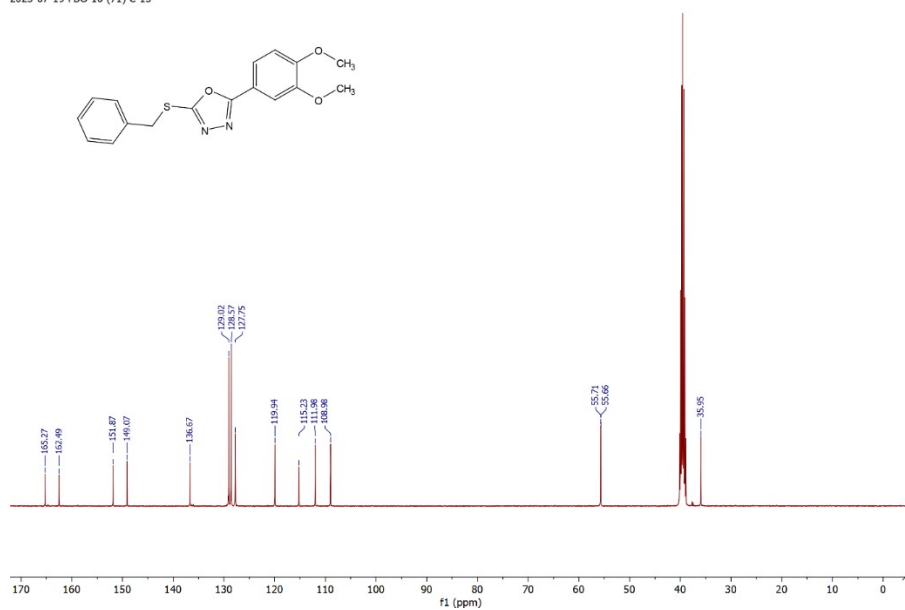
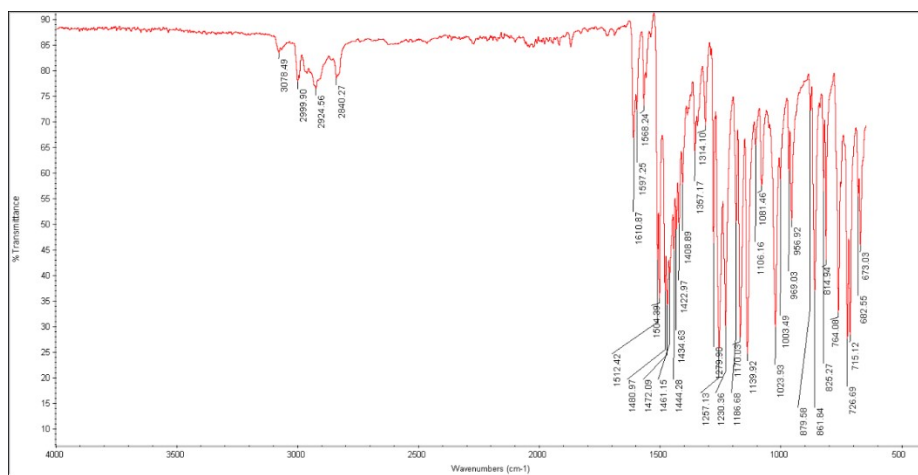
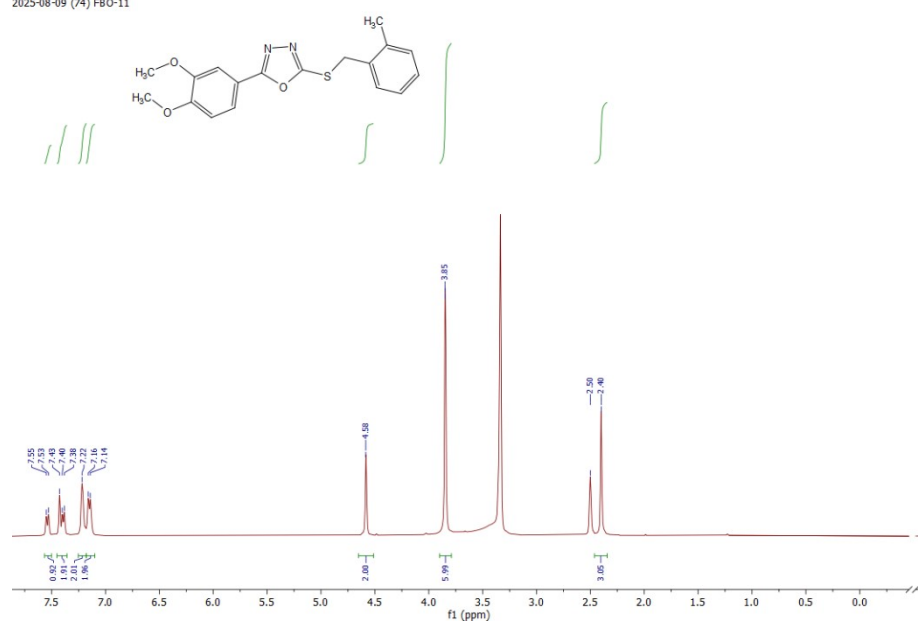


Figure S14: FT-IR, ¹H-, and ¹³C-NMR spectra of compound 7b.



2025-08-09 (74) FBO-11.1.fid
2025-08-09 (74) FBO-11



2025-08-09 (74) FBO-11 C-13.1.fid
2025-08-09 (74) FBO-11 C-13

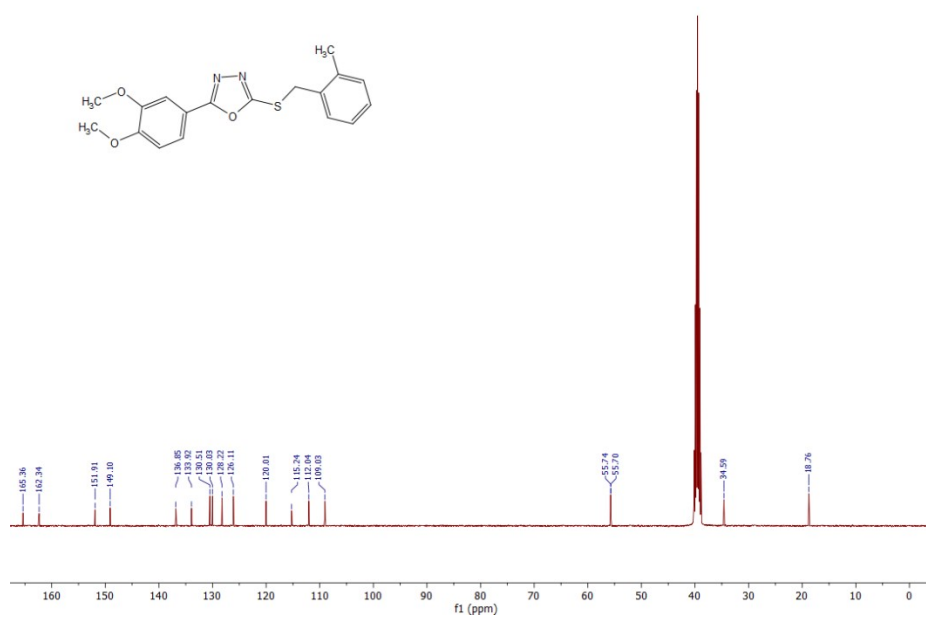
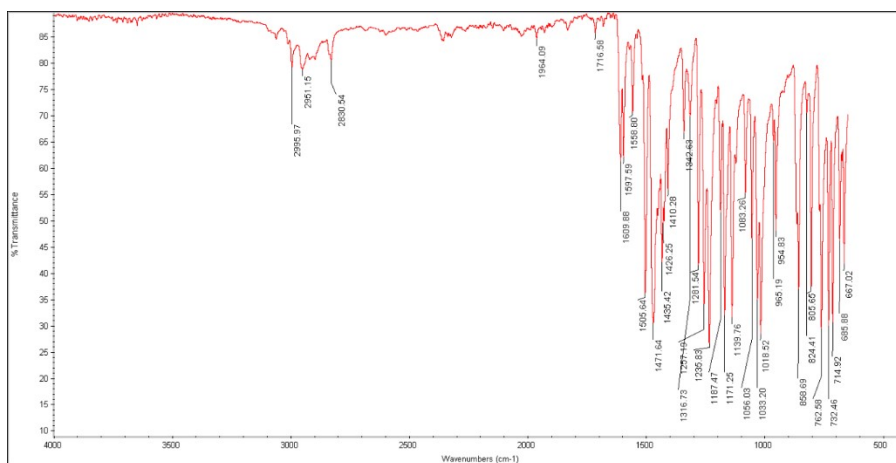
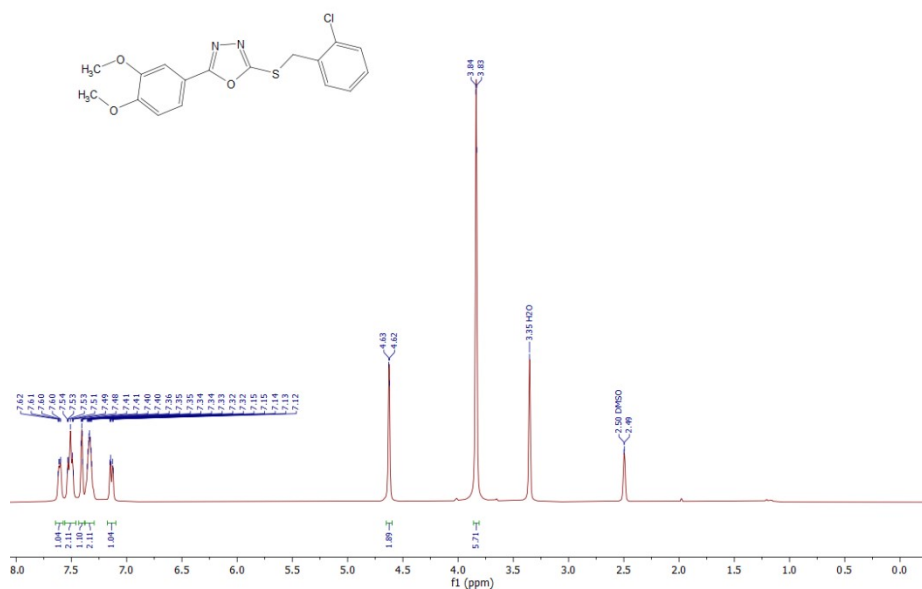


Figure S15: FT-IR, ^1H -, and ^{13}C -NMR spectra of compound 7c.



FB0-12 H-NMR.1.fid
FB0-12 H-NMR



FB0-12 C-13.1.fid
FB0-12 C-13

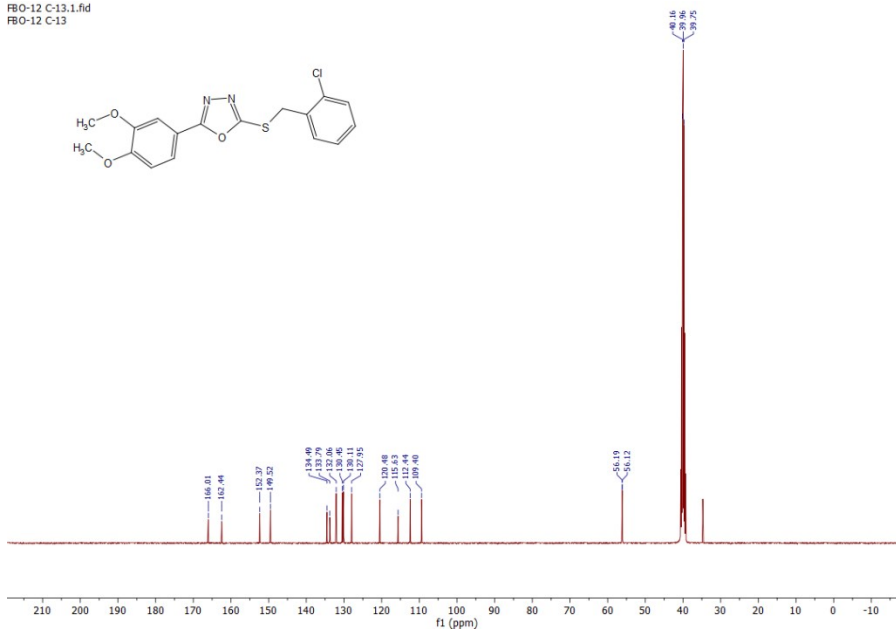
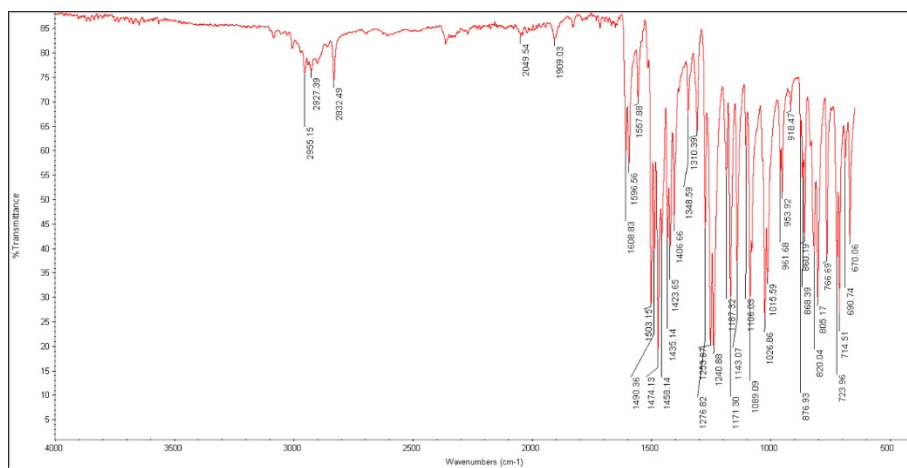
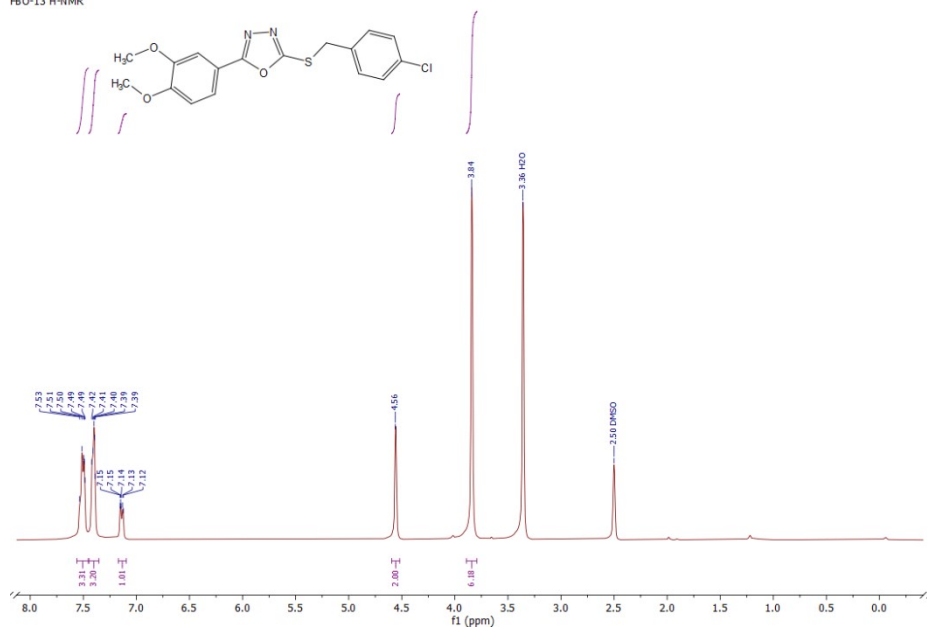


Figure S16: FT-IR, ^1H -, and ^{13}C -NMR spectra of compound **7d**.



FB0-13 H-NMR.1.fid
FB0-13 H-NMR



FB0-13 C-13.1.fid
FB0-13 C-13

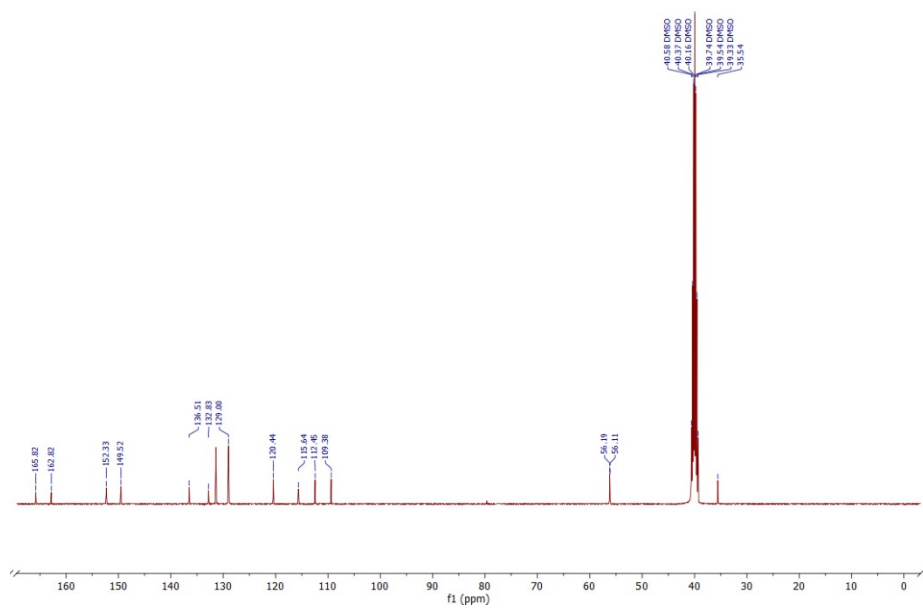
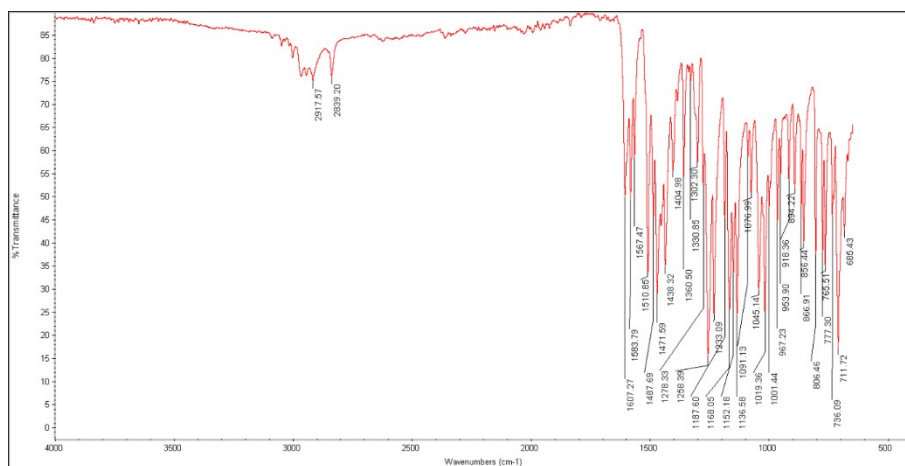
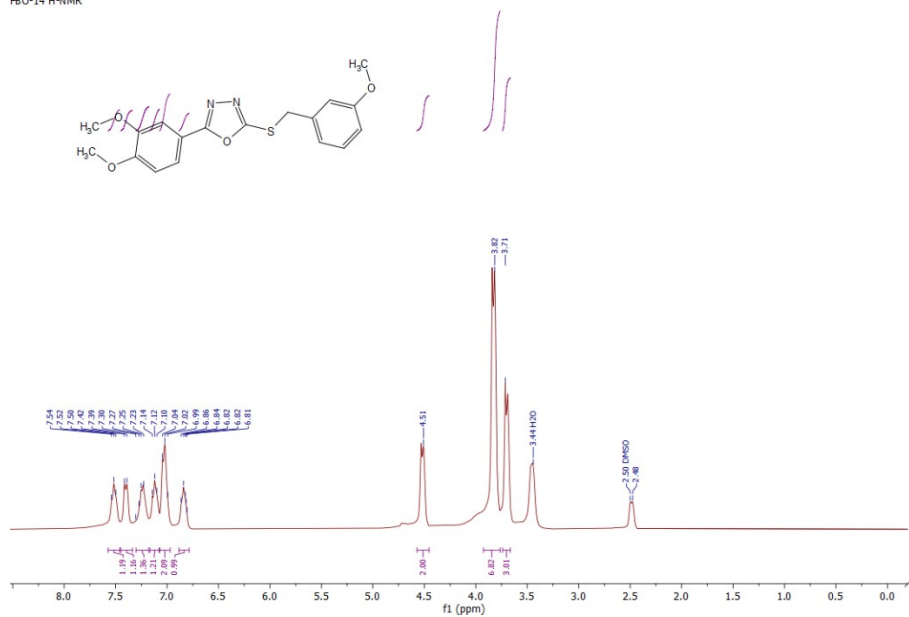


Figure S17: FT-IR, ¹H-, and ¹³C-NMR spectra of compound 7e.



FBO-14 H-NMR.1.fid
FBO-14 H-NMR



FBO-14 C-13.1.fid
FBO-14 C-13

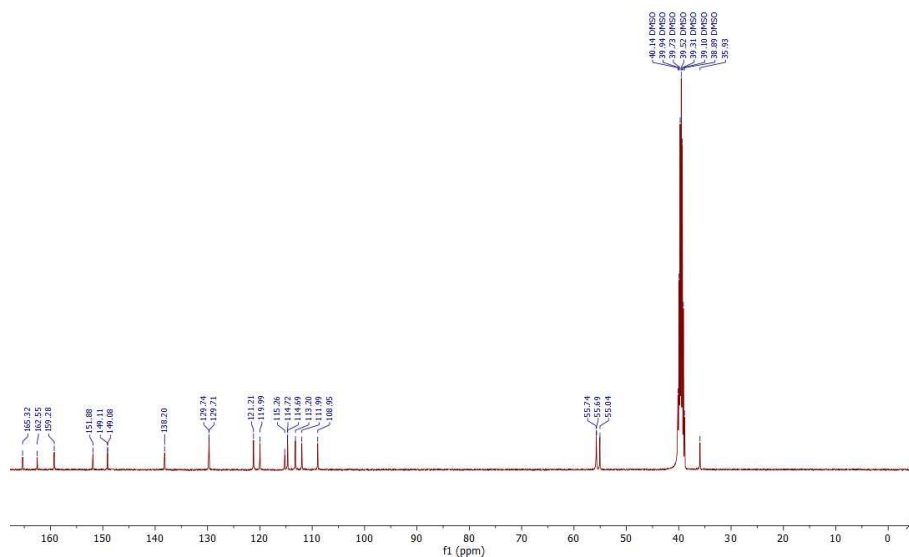
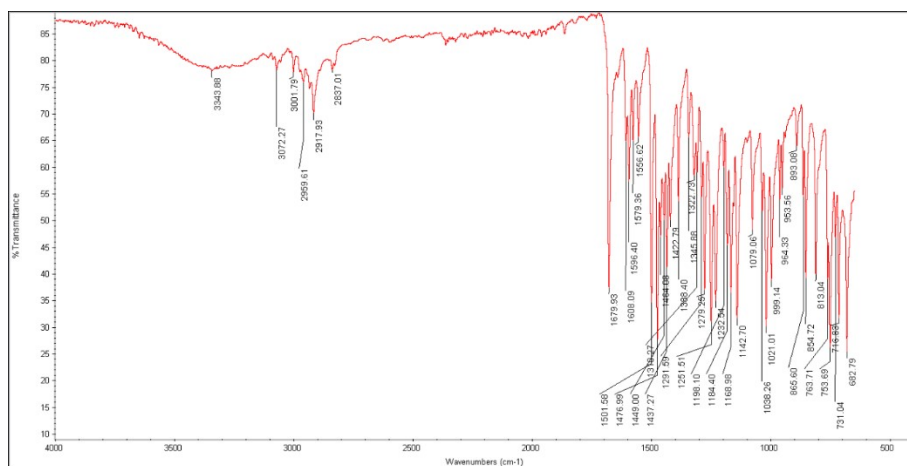
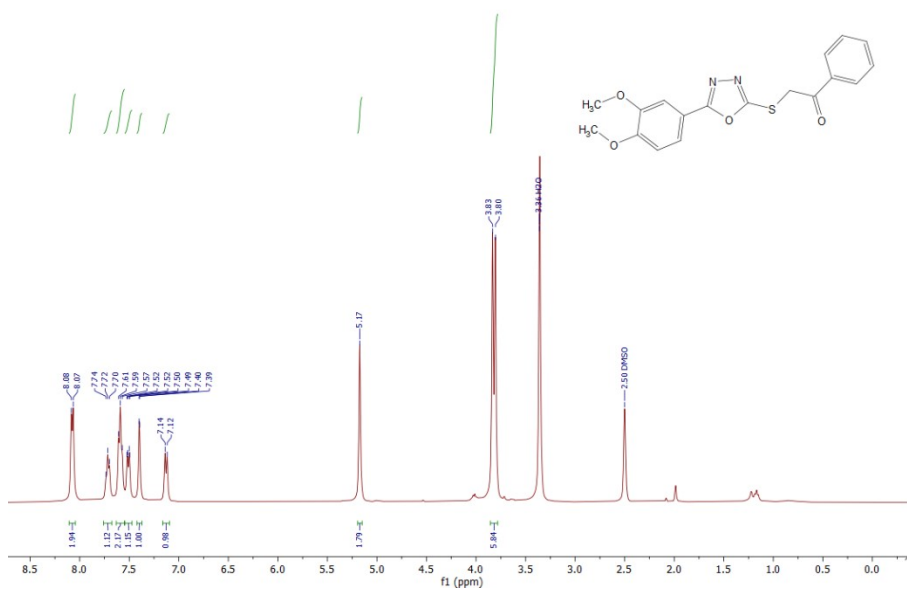


Figure S18: FT-IR, ¹H-, and ¹³C-NMR spectra of compound **7f**.



FBO-15 H-NMR.1.fid
FBO-15 H-NMR



FBO-15 C-13.1.fid
FBO-15 C-13

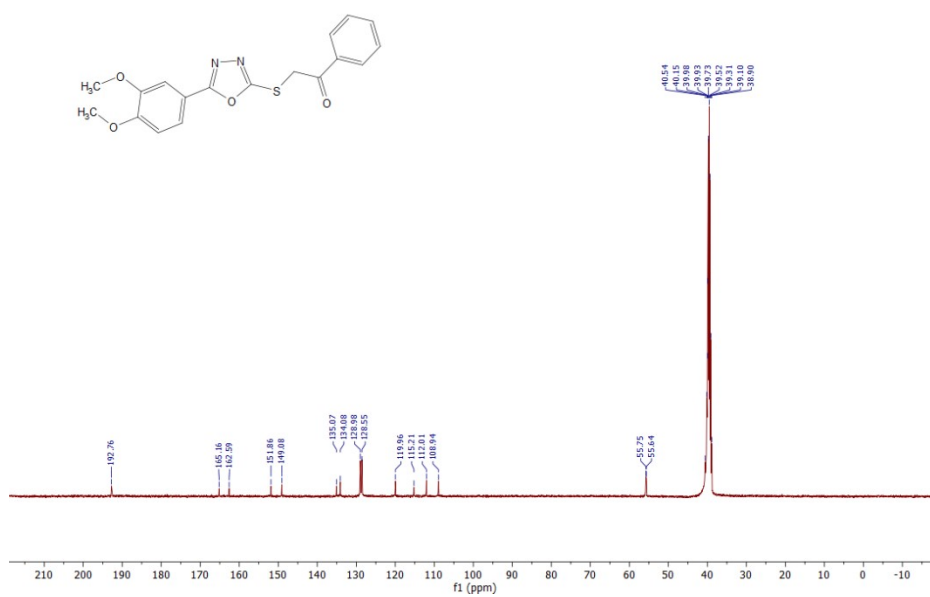


Figure S19: FT-IR, ¹H-, and ¹³C-NMR spectra of compound 7g.